Charge Dynamics and Spin Order in Doped Hubbard Models

Arno P. Kampf and Wolfram Brenig

Institut für Theoretische Physik, Universität zu Köln, Zülpicher Str. 77, 50937 Köln, Germany

Hole motion in an antiferromagnetic (AF) environment is accompanied by the emission of spin wave excitations. Spin-wave shakeoffs are responsible for incoherent contributions to the dynamics of propagating holes. Using a spin-density-wave polaron scheme we calculate the optical conductivity $\sigma(\omega)$ and show that the incoherent part of the hole spectrum contributes to the low-frequency part of $\sigma(\omega)$.

Separately, we discuss the possible formation of spiral spin patterns upon doping of the half-filled one-band Hubbard model. In particular, we consider the influence of band structure effects arising from nearest- and next-nearest-neighbor hopping processes on a square lattice. Differences in the ground state spin patterns for hole and electron doping are obtained offering a possible explanation for the persistence of AF order in low electron-doped cuprate superconductors.

PACS numbers: 75.10L, 75.30F, 75.30D.

1. INTRODUCTION

In the preceding article of this volume by Brenig and Kampf[1] a selfconsistent polaron scheme has been formulated to study the motion of a single hole in a spin-density-wave antiferromagnet. In this work results have been presented for the hole spectrum originating from the coupling to multiple spin-wave excitations. Extending the previous polaron analysis to finite hole concentrations we will discuss in the present article an example for the significance of the incoherent part of the spectrum. We will show that it creates oscillator strength in the low-frequency regime of the optical conductivity. Due to the magnetic origin of the incoherent part of the spectrum it is natural to argue that the spin fluctuations are responsible for optical absorption at mid-infrared frequencies.

In the second part of this article we investigate spiral spin structures in the one-band Hubbard model for densities away from half-filling. In these spiral states the staggered magnetization is not fixed along a certain direction but rather it slowly rotates with a wavenumber proportional to the density of doped carriers.[2] We extend earlier analyses of spiral states (see e.g. Ref.[3-7]) by including next-nearest-neighbor (t') hopping in the kinetic energy. On the Hartree-Fock level differences

in the groundstate spin patterns are found between hole and electron doping. In particular, for low electron doping concentrations commensurate AF remains stable over a finite concentration range near half–filling. This is compatible e.g. with the observed commensurate magnetic correlations in Ce doped Pr_2CuO_4.[8]

2. OPTICAL CONDUCTIVITY

The conductivity describes the response of the total current to an externally applied electromagnetic vector potential. We therefore consider the one–band Hubbard model in the presence of a time–dependent vector potential $A_x(\mathbf{r},t)$ applied in the x–direction, $\mathbf{r}$ denotes a site on the square lattice. The presence of the vector potential modifies the hopping term $c^+_{i+x}c_{ix}$ in the kinetic energy by introducing a Peierls phase factor $\exp(ieA_x(\mathbf{r},t))$. After expanding the kinetic energy to second order in $A_x(\mathbf{r},t)$ standard linear response theory leads to the formula for the complex, frequency dependent conductivity

$$\sigma_{xx}(z) = \frac{e^2}{iz}\left(C^r_{xx}(z) + \langle H^x_{kin}\rangle\right) . \tag{1}$$

Here, $z = \omega + i\delta$ and $\langle H^x_{kin}\rangle$ is the expectation value of the kinetic energy per site from hopping along the x–direction. $C^r_{xx}(\omega + i\delta)$ is the retarded current–current correlation function

$$C^r_{xx}(\omega + i\delta) = \frac{i}{N}\int_0^\infty e^{i(\omega+i\delta)t}\,dt\left\langle \left[J^P_x(t), J^P_x(0)\right]_- \right\rangle , \tag{2}$$

for the paramagnetic current operator $J^p_x = iet\sum_{i\sigma}(c^+_{i+x,\sigma}c_{i,\sigma} - c^+_{i,\sigma}c_{i+x,\sigma})$. The real part of the optical conductivity can be split into the Drude and a regular finite frequency part according to

$$Re\,\sigma_{xx}(\omega + i\delta) = D\delta(\omega) + \sigma_{reg}(\omega) = D\delta(\omega) + \frac{e^2}{\omega}\,Im\,C^r_{xx}(\omega + i\delta) , \tag{3}$$

where the Drude weight is given by $D = -\pi e^2\,Re\,C^r_{xx}(\omega \to 0 + i\delta) - \pi e^2\langle H^x_{kin}\rangle$. The regular part σ_{reg} of the conductivity is generally present in both metallic and

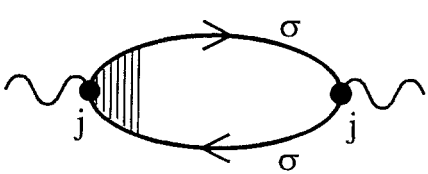

Fig. 1. Schematic diagram for the calculation of the current-current correlation function. Black circles indicate the coupling to the current and the set of vertical lines represents the current vertex function Γ_c.

insulating systems and arises from the electromagnetic field induced transitions to excited states. The Drude weight D of the δ–function at zero frequency is a consequence of the free acceleration of the quasiparticles. This is possible because the Hubbard model at zero temperature contains no dissipative mechanism, which would e.g. arise in the presence of disorder or from a coupling to phonons.

In the following we consider the charge dynamics of the spin–fluctuation dressed quasiparticles for which we evaluate $\sigma_{reg}(\omega)$. We use the polaron scheme for the Green's functions of the holes in the SDW limit of the Hubbard model as outlined in the article by Brenig and Kampf in this volume.[1] The required current–current correlation function C_{xx} for the renormalized SDW quasiparticles is calculated from the general diagram shown in Fig. 1. The result for the current correlator is written in the form

$$\begin{aligned} C_{xx}(\omega) &= i\frac{1}{N}\sum_{\mathbf{k}\sigma}\int\frac{d\nu}{2\pi}\Gamma_c(\mathbf{k},\omega,\nu)\Big[\big\{G^{11}_\sigma(\mathbf{k},\nu)G^{11}_\sigma(\mathbf{k},\omega+\nu)+G^{-1-1}_\sigma(\mathbf{k},\nu) \\ &\quad G^{-1-1}_\sigma(\mathbf{k},\omega+\nu)\big\}\,n^2(\mathbf{k},\mathbf{k})+\big\{G^{11}_\sigma(\mathbf{k},\nu)G^{-1-1}_\sigma(\mathbf{k},\omega+\nu)+ \\ &\quad G^{-1-1}_\sigma(\mathbf{k},\nu)G^{11}_\sigma(\mathbf{k},\omega+\nu)\big\}\,m^2(\mathbf{k},\mathbf{k})\Big]\gamma(\mathbf{k})\,. \end{aligned} \tag{4}$$

In Eq. 4 $\Gamma_c(\mathbf{k},\omega,\omega')$ is the current vertex function which includes the effects of repeated interactions between excited particle–hole pairs and $\gamma(\mathbf{k}) = \partial\epsilon(\mathbf{k})\partial k_x = 2t\sin k_x$. The coherence factors $m(\mathbf{k},\mathbf{k}')$ and $n(\mathbf{k},\mathbf{k}')$ are given by

$$m^2(\mathbf{k},\mathbf{k}') = v^+_{\mathbf{k}}v^-_{\mathbf{k}'}+v^-_{\mathbf{k}}v^+_{\mathbf{k}'} \qquad n^2(\mathbf{k},\mathbf{k}') = v^+_{\mathbf{k}}v^+_{\mathbf{k}'}-v^-_{\mathbf{k}}v^-_{\mathbf{k}'} \tag{5}$$

with $v^{+(-)}_{\mathbf{k}}$ as defined in Ref.[1] In Eq. 4 we have omitted already those terms which involve the interband Green's functions $G^{-1\,1}$ and $G^{1\,-1}$ because we will make use of the SDW polaron results in the large U/t limit for which the Green's function matrix $G^{ll'}$ becomes diagonal. Furthermore, we neglect vertex corrections which amounts to the replacement of $\Gamma(\mathbf{k},\omega,\nu)$ by $\gamma(\mathbf{k})$. Assuming that the SDW order is approximately preserved for a small but finite hole density we introduce a finite chemical potential into the Green's functions G^{ll}. This is somewhat similar to a rigid band calculation, but we emphasize that the Green's functions contain the full incoherent background contributions from the spin–fluctuation dressing.

The results of this calculation are shown in Fig. 2 for the regular part of the optical conductivity at different hole doping concentrations δ. At half–filling, $\delta = 0$, there is a gap to optical excitations across the insulating energy gap of the renormalized SDW state. For finite δ oscillator strength appears inside the gap. The corresponding spectral weight is removed from the high–energy interband contributions and shifted to low frequencies. The sharpness of the peak near $\omega = 0$ in Fig. 2 (which is *not* related to the Drude δ–function contribution omitted in this plot of σ_{reg} for frequencies $\omega > 0$) is a density of states effect and due to the flat quasiparticle dispersion along the magnetic Brillouin zone boundary.[1]

The optical absorption at low frequencies is entirely due to the spin–fluctuation dressing of the quasiparticles, i.e. the incoherent part of the propagator. Coherent particle–hole excitations in the valence band at finite hole doping contribute only to the zero–frequency Drude weight. In a rigid band picture for the Hartree–Fock SDW

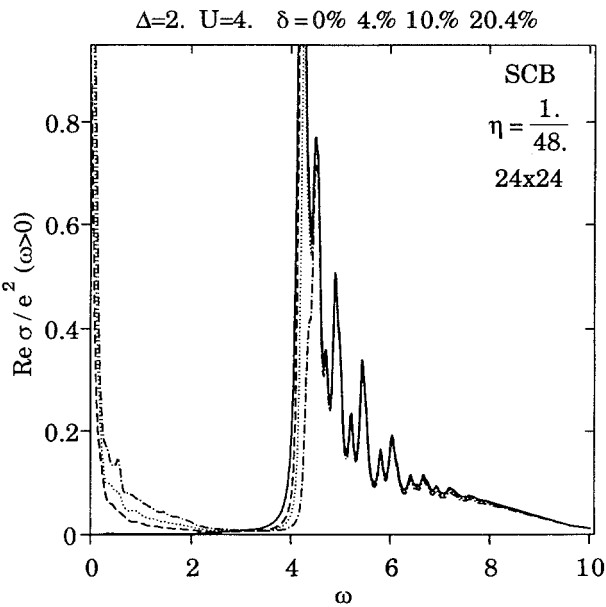

Fig. 2. Regular part σ_{reg} of the optical conductivity. The different curves correspond to hole concentrations $\delta = 0\%$ (solid line), 4% (dashed line), 10% (dotted line), and 20.4% (dashed–dotted line). This result has been obtained on a 24×24 lattice, with a finite imaginary part $i\eta = i/48$ added to the frequency ω for better convergence.

quasiparticles the regular part of $Re\,\sigma(\omega)$ would therefore contain only high–energy interband contributions. We may therefore directly identify the low–frequency optical conductivity with the spin fluctuations accompanying the doped holes. This provides a possible explanation for the origin of the so–called mid–infrared band observed in lightly doped cuprate superconductors.[9]

3. SPIRAL STATES

In this chapter we consider the separate problem of the ground–state spin structure in the one–band Hubbard model doped away from half–filling. Specifically, we discuss a Hartree–Fock treatment of spiral spin states which have been suggested to replace the commensurate antiferromagnetism realized at half–filling even in the presence of t'–hopping above a critical U.[10] For each lattice site i we assign a unit vector $\hat{\mathbf{n}}_i$ pointing in the direction, or opposite direction, of the on–site magnetization, depending on the different sublattices. $\hat{\mathbf{n}}_i$ is chosen as the local spin quantization axis as specified by the two spherical angles $\Omega_i = (\theta_i, \phi_i)$. With the unitary transformation[11,5,7]

$$d_{i\sigma} \equiv \sum_{\sigma'} [\mathcal{R}(\Omega_i)]_{\sigma\sigma'} = \sum_{\sigma'} \left[e^{i(\theta_i/2)\sigma_y} e^{i(\phi_i/2)\sigma_z} \right]_{\sigma\sigma'} c_{i\sigma'} \tag{6}$$

the Hubbard Hamiltonian takes a form which explicitly accounts for the new set of local spin quantization axes :

$$H(\{\Omega_i\}) = -t \sum_{\langle ij\rangle \sigma_1\sigma_2} \left(d^+_{i\sigma_1} \left[\mathcal{R}(\Omega_i)\mathcal{R}^+(\Omega_j)\right]_{\sigma_1\sigma_2} d_{j\sigma_2} + h.c. \right) + U \sum_i d^+_{i\uparrow} d_{i\uparrow} d^+_{i\downarrow} d_{i\downarrow}. \quad (7)$$

The Hubbard U term is naturally invariant under the unitary transformation Eq. 6. The subset of homogeneous spiral phases which preserve the discrete translational symmetry of the lattice is selected by the choice of the angles

$$\phi_i = 0 \qquad\qquad \theta_i = \mathbf{q}^S \cdot \mathbf{R}_i \quad (8)$$

where the wavenumber $\mathbf{q}^S$ characterizes the pitch of the spiral. This choice restricts the spiral arrangements of the magnetic moments into the $x-z$ plane, i.e. $\langle \mathbf{S}_i \rangle = m\,(\sin(\mathbf{q}_S \cdot \mathbf{R}_i), 0, \cos(\mathbf{q}_S \cdot \mathbf{R}_i))$ where m is the sublattice magnetization.

In the new local set of spin quantization axes the interaction term can be decoupled in the standard way. Introducing $\langle n^d_{i\sigma} \rangle = \frac{1}{2}n + \sigma m$, we look for solutions with a uniform hole density. The diagonalized Hartree–Fock Hamiltonian leads to two quasiparticle bands with the dispersion

$$E^{\pm}(\mathbf{k}) = \epsilon^+_{\mathbf{k}} \pm \sqrt{(\epsilon^-_{\mathbf{k}})^2 + (Um)^2} \quad (9)$$

where

$$\begin{aligned} \epsilon^{\mp}_{\mathbf{k}} \;=\; & -t \sum_{\alpha=x,y} \left(\cos(k_\alpha - \frac{q^S_\alpha}{2}) \mp \cos(k_\alpha + \frac{q^S_\alpha}{2}) \right) + \\ & -2t' \left(\cos(k_x - \frac{q^S_x}{2}) \cos(k_y - \frac{q^S_y}{2}) \mp \cos(k_x + \frac{q^S_x}{2}) \cos(k_y + \frac{q^S_y}{2}) \right). \quad (10) \end{aligned}$$

Here, we have included nearest–neighbor (t) as well as next–nearest–neighbor (t') hopping in the kinetic energy. The corresponding free energy has to be minimized with respect to the magnetization m and the spiral wave vector $\mathbf{q}^S$ for fixed density n. The Hartree–Fock quasiparticle dispersion of the commensurate SDW state is included in Eq. 9 for $\mathbf{q}^S = (\pi, \pi)$.

The mean–field U/t vs. filling phase diagram has a series of transitions between different spiral phases characterized by the wavenumber $\mathbf{q}^S$.[6,7] Fig. 3 shows the Hartree–Fock results for $\mathbf{q}^S$ as a function of filling for a fixed value of $U/t = 12$. $t'/t = -0.16$ has been chosen to model the band structure and the Fermi surface of the 214 cuprate materials. As is true in the absence of t'–hopping,[7] for arbitrarily small hole doping the commensurate AF state is found to be unstable against the diagonal spiral where $\mathbf{q}^S = q(1,1)$. The deviation of $\mathbf{q}^S$ from (π, π) starts out linearly with the hole dopant concentration. At a critical, U dependent doping $n_c(U)$, a 1^{st} order transition occurs to a $(1,0)$ spiral for which $\mathbf{q}^S = (Q, \pi)$.

The situation is different for electron doping. In this case the commensurate AF state is found to be stable against spiral distortions for a finite range of electron doping concentrations. A $(1,1)$ spiral state appears above a critical U dependent $n_c > 1$. This asymmetry between hole and electron doping arises here obviously

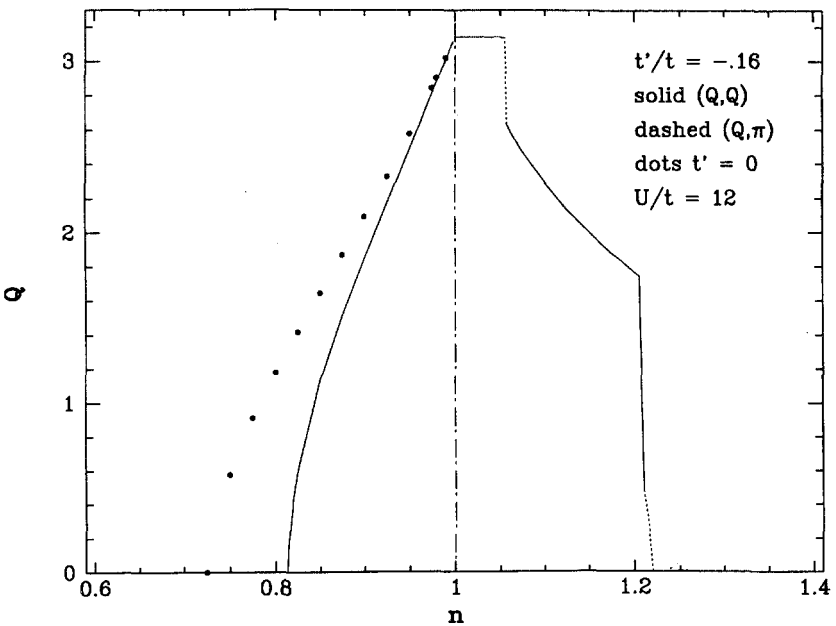

Fig. 3. Hartree–Fock spiral wavenumber Q as a function of hole or electron doping concentration away from half-filling for the parameters $U/t = 12$ and $t'/t = -0.16$. Black dots (•) indicate the corresponding results for $t' = 0$. Solid lines represent the diagonal (1,1) spiral with $\mathbf{q}^S = (Q, Q)$ and the dashed line represents the transverse spiral with $\mathbf{q}^S = (Q, \pi)$.

from a band structure effect due to the inclusion of t'–hopping. Besides microscopic differences between hole and electron doping of the CuO_2 planes, this result provides another possible origin for the robustness of the commensurate Néel order in the electron doped 214 materials.[12] It also agrees with the neutron scattering data which show that the magnetic correlations in Pr_2CuO_4 remain commensurate under Ce doping which adds electrons to the CuO_2 planes.[8]

Is is tempting to relate the incommensurate spin modulation of the spiral states with the splitting of the magnetic peak seen in the neutron scattering data for $La_{2-x}Sr_xCuO_4$. The experimentally observed discommensuration would correspond to the wavenumber of the (1,0) spiral state. This connection has been made on the basis of a more sophisticated slave boson treatment.[6] The obtained energies for the spiral states in the slave boson formulation agree within 2% with QMC results indicating that spiral states are good approximate candidates for the ground state of the Hubbard model near half-filling and at intermediate to large values of U/t.[6]

ACKNOWLEDGEMENT

It is a pleasure to acknowledge encouraging discussions with E. Müller–Hartmann and G.A. Thomas. This work has been performed within the program of the Sonderforschungsbereich 341 supported by the Deutsche Forschungsgemeinschaft.

REFERENCES

1. W. Brenig and A. P. Kampf, previous article in this volume and *Europhys. Lett.* **24**, 679 (1993)
2. B.I. Shraiman and E.D. Siggia, *Phys. Rev. Lett.* **62**, 1564 (1989); *Phys. Rev. B* **40**, 9162 (1989)
3. C. Jayaprakash, H.R. Krishnamurty, and S. Sarker, *Phys. Rev. B* **40**, 2610 (1989)
4. C.L. Kane, P.A. Lee, T.K. Ng, B. Chakraborty, and N. Read, *Phys. Rev. B* **41**, 2653 (1990)
5. E. Arrigoni and G.C. Strinati, *Phys. Rev. B* **44**,7455 (1991)
6. R. Frésard and P. Wölfle, *J. Phys. Condensed Matt.* **4**, 3625 (1992); M. Dzierzawa, *Zeitschrift für Physik B* **86**, 49 (1992); R. Frésard, M. Dzierzawa, and P. Wölfle, *Europhys. Lett.* **15**, 325 (1991)
7. F.F. Assaad, *Phys. Rev. B* **47**, 7910 (1993)
8. T.R. Thurston, M. Matsuda, K. Kakurai, K. Yamada, Y. Endoh, R.J. Birgeneau, P.M. Gehring, Y. Hidaka, M.A. Kastner, T. Murakami, and G. Shirane, *Phys. Rev. Lett.* **65**, 263 (1990)
9. S. Uchida, T. Ido, H. Takagi, T. Arima, Y. Tokura, and S. Tajima, *Phys. Rev. B* **43**, 7942 (1991)
10. H.Q. Lin and J.E. Hirsch, *Phys. Rev. B* **35**, 3359 (1987)
11. Z.Y. Weng and C.S. Ting, *Phys. Rev. B* **42**, 803 (1990)
12. B. Keimer, A. Aharony, A. Auerbach, R.J. Birgeneau, A. Cassanho, Y. Endoh, R.W. Erwin, M.A. Kastner, and G. Shirane, *Phys. Rev. B* **45**, 7430 (1992)